IEEE Access
Multidisciplinary | Rapid Review | Open Access Journal

Received December 26, 2016, accepted January 24, 2017, date of publication January 30, 2017, date of current version March 13, 2017.

Digital Object Identifier 10.1109/ACCESS.2017.2661278

Low-Profile and Wide-Beamwidth Dual-Polarized Distributed Microstrip Antenna

XI CHEN[1], (Member, IEEE), PEI-YUAN QIN[2], (Member, IEEE), Y. JAY GUO[2], (Fellow, IEEE), AND GUANG FU[1]

[1]National Key Laboratory of Antennas and Microwave Technology, Collaborative Innovation Center of Information Sensing and Understanding, Xidian University, Xi'an 710071, China
[2]Global Big Data Technologies Centre, University of Technology Sydney, Ultimo, NSW 2007, Australia

Corresponding author: X. Chen (xchen@mail.xidian.edu.cn)

This work was supported in part by the National Natural Science Foundation of China under Grant 61601351 and in part by the Fundamental Research Funds for the Central Universities under Grant JB160201, and in part by the Australian Research Council Discovery Project under Grant DP160102219 and DECRA under Grant DE170101203.

ABSTRACT A low-profile and wide-beamwidth dual-polarized distributed microstrip antenna is presented in this paper. Four isolated micro patches are proposed as the radiation components and are excited by a compact differential-fed network. The micro patches in two diagonals determine the operating frequency bands of the two polarizations, respectively. By increasing the distances between the micro patches, the beamwidth in E plane can be broadened. Shorting poles between the patches and the ground plane are used to achieve good impedance matching. Compact dual-polarized differential-fed networks are also studied and compared with achieve the best antenna performance. To validate the proposed method, a wide-beamwith dual-polarized distributed microstrip antenna, whose dual polarizations operate at 2 and 2.2 GHz, respectively, is manufactured and measured. The external dimensions of the antenna is 70mm$\times$10mm ($0.49\lambda\times0.07\lambda$). The experimental results agree well with the simulated ones. The 3dB beamwidths in E planes reach 116° and 115°, and the gains are 5.15 and 5.5 dB for two polarizations, respectively. Meanwhile, the cross polarizations are less than -26.2 and -27.8 dB. In addition, the impedance bandwidths of 9.2% and 9.9% for VSWR$\leq$2 are achieved, and the port isolation is greater than 25.4 dB in the bands.

INDEX TERMS Distributed microstrip antenna, dual polarization, low profile, wide beamwidth, differential feed.

I. INTRODUCTION

Dual-polarized antennas have been widely used in wireless communications and imaging radar systems [1]–[6]. They can help increase the polarization diversity of the system and reduce the number of the antenna elements used [7]. When employed on a mobile communication platform, dual-polarized antennas are required to be compact and light. This is particularly true for antennas mounted on high-speed aircrafts, where the low profile of the antenna is a crucial feature to reduce the effect of protrusion on the aerodynamic performance of the aircrafts. Furthermore, owing to the quick change of the aircraft attitude, a wide beamwidth of the antenna is also required to maintain reliable communication links.

The realization of compact dual-polarized antennas typically resorts to the following approaches: crossed dipoles [1], [2], [8], [9], magneto-electric dipoles [10]–[12], magnetically coupled patch antennas [13], [14], and microstrip antennas [15], [16]. Crossed dipoles are normally placed above a reflecting plate whose diameter is usually $0.5\sim1\lambda$ (λ is the free-space wavelength of the operating frequency). For a high-gain or wide-beamwidth radiation, the height of the crossed dipoles from plate is usually $0.25\sim0.5\lambda$. Although this configuration is not low profile, it is still widely used in fixed base-station antennas due to its wideband and low-cost advantages [8], [9]. Dual-polarized magneto-electric dipole is an evolution type of the crossed dipoles, which introduces the equivalent magnetic-current structure to improve the symmetry and front-to-back ratio of the radiation patterns [10]–[12], and the dimensions of the antenna are similar to those of the crossed dipoles. In [12], it is shown that employing dielectric loading can reduce the height of the dual-polarized magneto-electric dipole to 0.15λ. Dual-polarized magnetically coupled patch

antennas are recently reported in [13] and [14], which adopt magnetic coupling to solve the impedance matching problem of the low-height (0.15λ) patch antennas. For low-profile applications at lower microwave frequencies, however, the heights of above antennas may not be acceptable. In general, dual-polarized microstrip antennas can be made low-profile and are suitable for conformal designs, but the bandwidth tends to decrease with the antenna height. Furthermore, there is little flexibility in controlling the radiation performance of the low-height microstrip antennas such as the 3dB beamwidth and gain [15], [16].

Increasing the beamwidth of microstrip antennas can improve the coverage of communications systems [17]–[21]. There are two well-known approaches to increasing the beamwidth of microstrip antennas. The first one is to employ thick and high-permittivity substrates to increase the surface wave in the horizontal direction. Unfortunately, this may lead to an increase in antenna losses and reduction in the bandwidth [17], [18]. Also, it may increase the cost of the antenna. The second approach is to reshape the radiation patch and the ground plane to increase the radiation at low-elevation angles. However, this approach will increase the total length and height of the antenna, which sacrifices the low-profile advantage of microstrip antennas [19]–[21]. Therefore, it is very challenging to design a low-profile antenna with a wide beamwidth. To the best of the authors' knowledge, there have been very few reports on low-profile antennas with both dual polarization and wide beamwidth.

In this paper, a novel low-profile dual-polarized distributed microstrip antenna is presented. Different from traditional microstrip antennas, the antenna is composed of four distributed and differentially fed micro patches that can generate a wide beamwidth of the radiation pattern and dual polarizations. The total size of the four micro patches is no more than 0.36λ×0.36λ which is far smaller than a four-element microstrip array. By adjusting the relative parameters of the micro patches, satisfactory bandwidths are also obtained respectively for the two orthogonal polarizations.

The contributions of the paper can be summarized as follows: 1) A low-profile, wide-beamwidth dual-polarized antenna is proposed. To our knowledge, this is the first reported antenna of its kind; 2) A novel distributed and differentially fed microstrip antenna is proposed, which enables the flexible design of low-profile antennas; 3) A new method to control the beamwdith of microstrip antennas is proposed, which does not resort to increasing antenna dimensions or using high-permittivity substrates. In the following sections, the basic antenna structure and the principle of the differential feed are presented first in section II. The properties of the antenna are analyzed and discussed in section III. In section IV, combining with the proposed antenna, three types of compact dual-polarized differential-fed networks are analyzed and compared. In section V, a low-profile and wide-beamwidth dual-polarized distributed microstrip antenna is designed, experimented and discussed. At last, the paper is summarized in section VI.

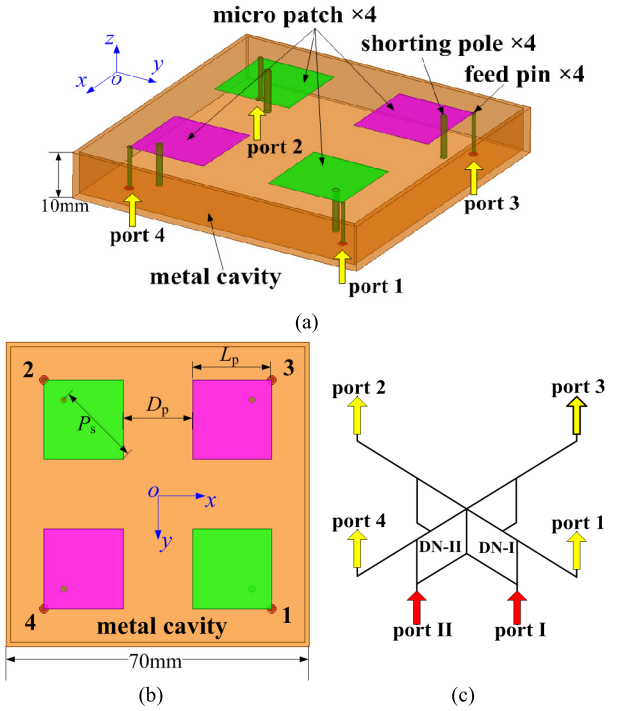

FIGURE 1. Configuration of the antenna. (a) 3D view. (b) Top view. (c) Sketch of the dual-polarized differential-fed networks.

II. ANTENNA STRUCTURE AND PRINCIPLE

A. CONFIGURATION OF THE ANTENNA

The basic structure of the proposed antenna is shown in Fig. 1(a). The antenna consists of four micro patches, four feed pins, four shorting poles and a square metal cavity. The micro patch is a small square metal patch, whose length, labeled as L_p, is in the range of 0.1∼0.2λ. Four micro patches are placed symmetrically in the square metal cavity. The height of the micro patches from the bottom of the square cavity is less than 0.1λ, labeled as H_p. The side-to-side distance between the micro patches is labeled as D_p. By adjusting D_p, the radiation property of the antenna can be changed. The micro patches are fed through the feed pins. The tops of the feed pins are connected to the outer corners of the four micro patches, i.e. those close to the four corners of the cavity, and the bottoms of the pins are connected to the excitation sources. The diameter of the pins is 1mm. As shown in Fig. 1(b), on the diagonal of each micro patch, a shorting pole is employed, which connects the micro patch to the square cavity and is used for impedance matching of the antenna. The position of the shoring poles is labeled as P_s. The radius of the shoring poles is labeled as r_s. The square cavity is located at the bottom of the antenna and surrounds the micro patches. The employment of the cavity can lessen the effect of the surrounding environment on the antenna performance. The length of cavity is labeled as L_c, and the height is also H_p. The wall thickness of the cavity is 1mm. Therefore, the external dimensions of the antenna is $L_c \times H_p$. In the design of this paper, $L_c \times H_p$ is made to be 70mm×10mm (0.49λ×0.07λ at 2.1GHz).

B. PRINCIPLE OF THE DIFFERENTIAL FEED

There are four exciting ports on the antenna, as shown in Fig. 1(a), which are labeled as port 1 ∼ port 4 respectively. When port 1 and port 2 are excited by using the differential feed, i.e. excited through the equal-amplitude and out-of-phase currents, the corresponding pair of the micro patches radiates one linear polarization. Similarly, when port 3 and port 4 are differentially excited, the other pair of the micro patches radiates another linear polarization which is orthogonal to that excited by ports 1 and 2. This way, dual linear polarizations are achieved. As shown in Fig. 1(c), by using a differentially-fed network (DN), port 1 and port 2 can merge into the differential port I, and port 3 and port 4 can merge into port II. Since the distances between the micro patches are very small, the strong coupling between them cannot be neglected. By virtue of references [10], [22], when using S parameters to express the energy transfer between the four micro patches, the reflection coefficients of the differential port I and port II can be derived from equation (1).

$$S_{I.I} = \frac{1}{2}(S_{11} - S_{12} - S_{21} + S_{22}) \tag{1a}$$

$$S_{II.II} = \frac{1}{2}(S_{33} - S_{34} - S_{43} + S_{44}) \tag{1b}$$

The coupling coefficients between the differential port I and port II can be derived from equation (2).

$$S_{II.I} = \frac{1}{2}(S_{31} - S_{41} - S_{32} + S_{42}) \tag{2a}$$

$$S_{I.II} = \frac{1}{2}(S_{13} - S_{14} - S_{23} + S_{24}) \tag{2b}$$

When the structures of the two micro patches in one diagonal are centrally and bilaterally symmetrical, in terms of the symmetry of the energy transmission between the four micro patches, equations (1) and (2) can be simplified into equations (3) and (3c) as follows, respectively.

$$S_{I.I} = S_{11} - S_{12} \tag{3a}$$

$$S_{II.II} = S_{33} - S_{34} \tag{3b}$$

$$S_{II.I} = S_{I.II} = 0 \tag{4}$$

Therefore, when the antenna structure is ideally symmetrical, the isolation between the two differential ports should be infinitely large. From equation (3), when the coupling coefficient (S_{12} and S_{34}) in one pair of the micro patches is small, the reflection coefficient of differential port ($S_{\mathrm{I.I}}$ and $S_{\mathrm{II.II}}$) is mainly determined by the reflection coefficient of the micro-patch port (S_{11} and S_{33}). Fig. 2 shows the S_{12} (S_{34}) and S_{13} (S_{31}) of the proposed antenna. The coupling coefficient (S_{12}& S_{34}) in one pair of the micro patches is less than −20dB in the operating band. In section III, the performance of the antenna under ideal excitations will be studied first, and then several compact dual-polarized differential-fed networks combining with the above antenna will be analyzed and discussed in section IV.

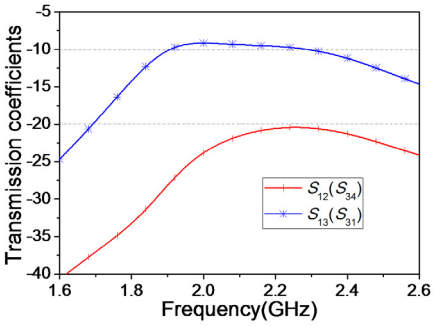

FIGURE 2. Transmission coefficients of the proposed antenna.

III. IMPEDANCE MATCHING, OPERATING FREQUENCY AND BEAMWIDTH

In order to clearly demonstrate the operating mechanism of the distributed microstrip antenna, the impedance matching, operating frequency and beamwidth of the antenna are analyzed through parametric studies.

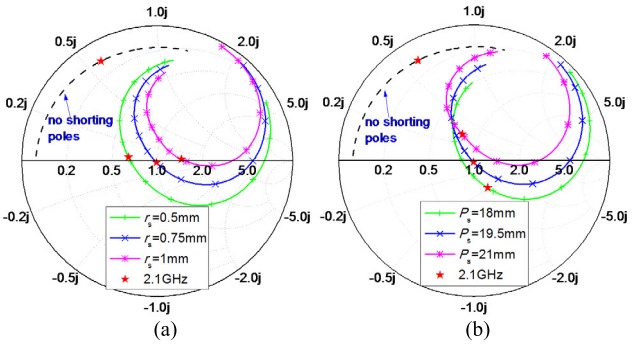

FIGURE 3. Effect of the shorting poles on the input impedance of micro patches. (a) Radius of the shoring pole. (b) Position of the shorting pole.

A. IMPEDANCE MATCHING

Owing to their small electrical sizes and the small distance from the ground plane, the input impedances of the micro patches present small resistance and pure inductance which are hard to be matched to the port impedance. As seen in Fig. 3, the dashed line in smith chart shows the input impedance of the micro patch without shorting poles. The shorting poles play an important role in impedance matching. By adjusting the radius and position of the shoring poles, good impedance matching can be achieved to the specified port impedance. Fig. 3 shows the variations of the input impedance with different radii and positions when the port impedance is equal to 100Ω. The 100Ω port impedance is determined by the requirement of the differential-fed network. It is observed, by adjusting the radius of the shorting pole, desired input resistance at resonant frequency (2.1GHz) can be achieved. By adjusting the position of the shorting poles, the input reactance can be made to zero from inductance or capacitance.

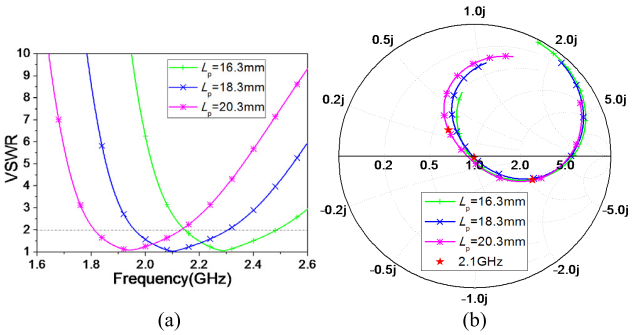

FIGURE 4. Effect of L_p on the operating frequency of the micro patches. (a) VSWR. (b) Input impedance.

B. OPERATING FREQUENCY

The effects of the length of the micro patch L_p on the resonant frequency are examined. Fig. 4(a) shows the VSWR curves when L_p is equal to 16.3mm, 18.3mm and 20.3mm, respectively. As can be seen, the operating frequency band decreases neatly when the length is increased. The best-matching frequencies are at 1.94GHz, 2.1GHz, 2.29GHz respectively. The bandwidths for VSWR$\leq$2 are stable with a relative bandwidth of about 16.5%. The corresponding input impedances are given in Fig. 4(b). The impedance curve circles nicely across the center of the smith chart as L_p changes. It is also indicated that the resonant frequency of the antenna can be controlled exactly. This property can be used to control the respective operating frequencies of the dual polarizations, which implies that the dual orthogonal polarizations can operate either at the same frequency or at different frequencies.

C. BEAMWIDTH

It is very challenging to control the beamwidth for conventional microstrip antennas because of the difficulty in manipulating the current distribution on the radiation aperture. For the proposed distributed microstrip antenna, however, beamwidth controlling can be achieved by adjusting the distance between the micro patches to change the superposition of the radiation fields from the micro patches. Fig. 5(a) shows the current distribution on the micro patches, feed pins and shorting poles. It is observed the current consists of the horizontal and vertical components (I_h & I_v), and the vertical currents on the pins and poles are same in phase. Fig. 5(b) shows the sum radiation pattern (RP) from the horizontal and vertical currents. The maximal value of the RP points to the direction of $\theta = 40°$ rather than the normal direction, which is a result of the tilted sum current I_{sum} of the two current components. This also indicates that the vertical current plays an important part on the radiation of the micro patch. Based on the current distribution, Fig. 5(c) shows the schematic diagram forming the wide beamwidth of the antenna. When one pair of patches are fed by equal-amplitude and out-of-phase excitations, the horizontal currents on the two micro patches are in phase, so the resultant radiation is always the strongest in the normal direction. On the other

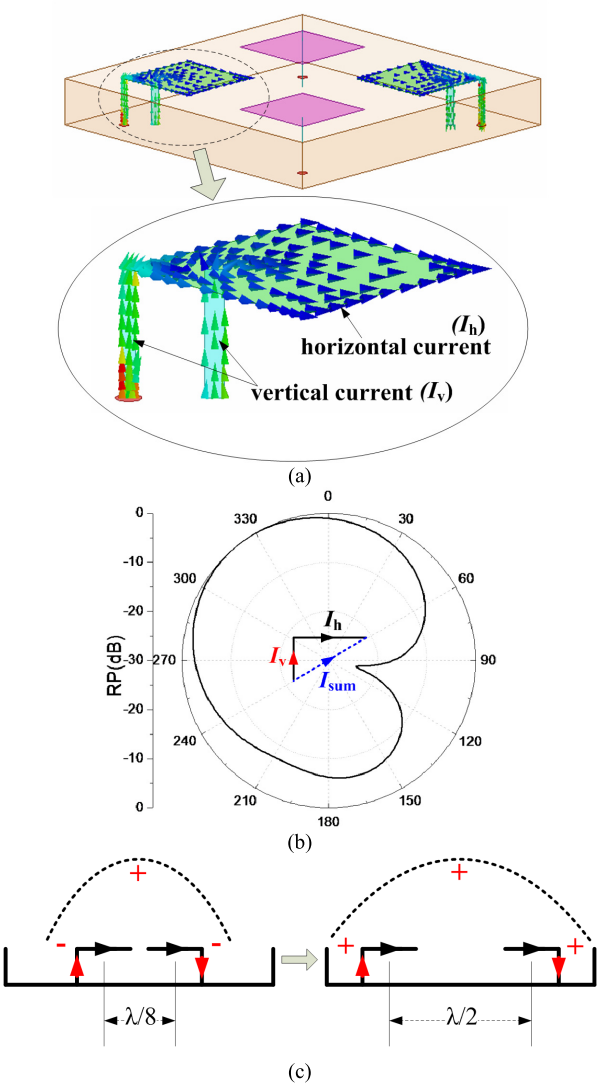

FIGURE 5. Principle of the wide beamwidth in the proposed antenna. (a) Current distribution. (b) RP of the micro patch. (c) Schematic diagram of the wide beamwidth.

hand, the vertical currents on one pair of feed pins are out of phase. When the distance between the micro patches is small, the radiation fields from the vertical components are approximately cancelled near the horizon. When the distance is around a half wavelength, the radiation fields from the vertical components will add constructively in the horizontal direction, thus broadening the beam.

Fig. 6 shows the variation of E-plane and H-plane radiation patterns at 2.1GHz when the distance D_p changes from 1mm to 16mm. It is observed the 3dB beamwidth in E plane increases with D_p. When D_p = 1mm, 8mm and 16mm, the corresponding 3dB beamwidth is 90°, 105° and 120°. While 3dB beamwidth in H plane has few change, and they are 95°, 97° and 98°. This is an unconventional and significant advantage compared to the previous reported dual-polarized antennas, whose beamwidth in E plane is usually less than that in H plane [8]–[19]. This method can make the

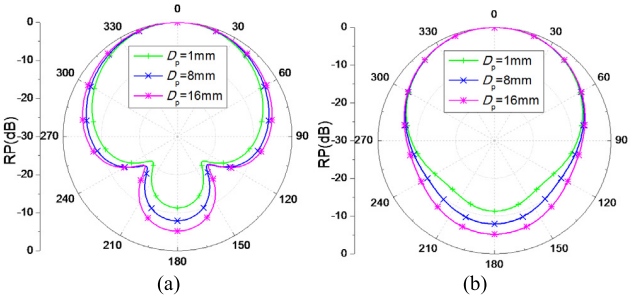

FIGURE 6. RPs with different D_p. (a) E plane. (b) H plane.

wide-beamwidth design more flexible for microstrip antennas without enlarging the antenna dimensions. Further, some parasitic strips could be added at both sides of each micro patch to control the beamwidth in H plane.

IV. DIFFERENTIAL FEED NETWORK

To excite a pair of micro patches with equal amplitude and 180° out of phase, a differential feed network should be employed. The performance of the differential feed network will affect the performance of the antenna, including the level of the cross polarization, impedance bandwidth and port isolation [10]. A traditional differential feed network includes rat-race coupler or power divider/3dB coupler with phase shifter [23], and they are all large in size. Usually, these networks can provide good bandwidths and isolations for dual-polarized antennas but also incur non-negligible insertion losses [15], [16]. In our design, the length of the proposed antenna is less than 0.5λ, so it is difficult to accommodate two differential feed networks in a conventional single-layer PCB. Therefore, low-loss and compact differential-fed networks are desired.

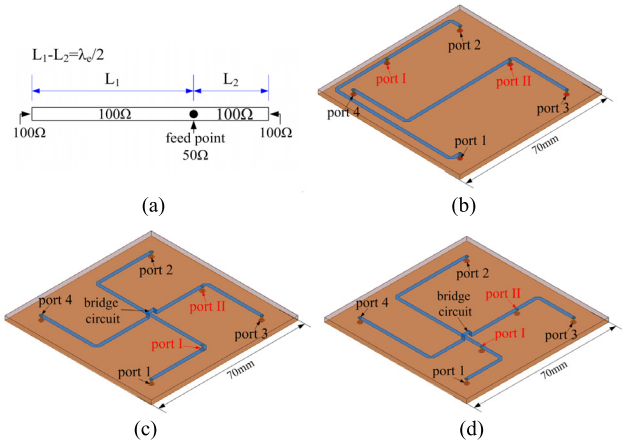

FIGURE 7. Dual-polarized differential-fed networks. (a) Schematic of the differential-fed line. (b) No-cross type. (c) Center-cross type. (d) Side-cross type.

The principle of the proposed differential feed network is shown in Fig. 7(a). It is a 100Ω transmission line with a feed point located at an appropriate position. When the two ends of the transmission line connect to the impedance of 100Ω, the input impedance of 50Ω can be achieved at the feed point without impedance transformer. The position of the feed point should make the output phases at two ends be 180° out of phase, so the smallest length of the entire transmission line is a half substrate wavelength. According to these rules, two microstrip differential-fed lines are designed on a 70mm×70mm×2mm substrate with a relative permittivity of 2.65 and a loss tangent of 0.002. The width of 100Ω microstrip line is about 1.5mm.

Three layouts of the dual-polarized differential-fed lines are constructed and compared. The first one is a no-cross type, shown in Fig. 7(b). To avoid the cross of the two lines, the differential-fed line I goes from the outside of the differential-fed line II. Due to the limited sizes of the substrate and the existence of the metal cavity, the two differential lines are close to each other in some parts. The second one is a center-cross type, shown in Fig. 7(c). The shapes and lengths of the two differential lines are same, and they cross at the center of the line. A bridge circuit is used to insulate the two lines. The length and height of the bridge is 3.5mm and 2mm respectively. In this type, the two lines are balanced and symmetric in layout, and the space between the lines is large. The third one is a side-cross type, shown in Fig. 7(d). To reserve the center area for the supporting structure, the cross position of the two lines is shifted off the center and located at the side. Here, the two lines are not symmetric, but the space between the lines is still large.

The three types of dual-polarized differential-fed networks are respectively calculated with the above antenna, and port 1 ∼ port 4 connect with the corresponding ports of the antenna. Fig. 8 and Fig. 9 present the RP in E plane, VSWR and the port isolation of the entire antenna. It is observed the cross polarization in no-cross type has the lowest value, which is −31.3dB at $\theta = 0°$. The values of the center-cross and side-cross types are −29.6dB and −29.3dB respectively. Due to the differential-fed lines, the impedance bandwidths of the antenna decrease in some degree. The bandwidths for VSWR≤2 are all in the range of 9.1%∼10.7% for the three types. The port isolation of the no-cross type is just more than 20dB in 2∼2.2GHz, while those in center-cross and side-cross types are more than 26.1dB and 25.9dB respectively. In addition, the gains of the three types are very close, and the 3dB beamwidths in E plane are all in the range of 118° ∼ 119°. These comparisons are all listed in Table 1. From these results, although adding a bridge circuit, the center-cross and side-cross types provide better dual-polarized properties than the no-cross one does in the compact structure. Meanwhile, the cross position has little effect on the antenna performance. Therefore, the side-cross one will be used in the design for the central reservation to supporting structure.

V. EXPERIMENT AND DISCUSSION

According to the above methods and structures, it is flexible to design a low-profile and wide-beamwidth dual-polarized antenna. In the above analysis, the four micro patches have

TABLE 1. Comparisons of the performance on the antenna with three types of dual-polarized differential-fed networks.

Terms	Gain (dB)	3dB-BW (°)	Cross-pol. (dB) @ θ=0°	Imp. Bandwidth		$S_{II,I}$ (dB) 2~2.2GHz
				Port 1	Port 2	
No-cross	5.13	118	-31.3	10.7%	9.1%	-20.6
Center-cross	5.14	119	-29.6	10.3%	9.7%	-26.1
Side-cross	5.12	118	-29.3	10.4%	9.5%	-25.9

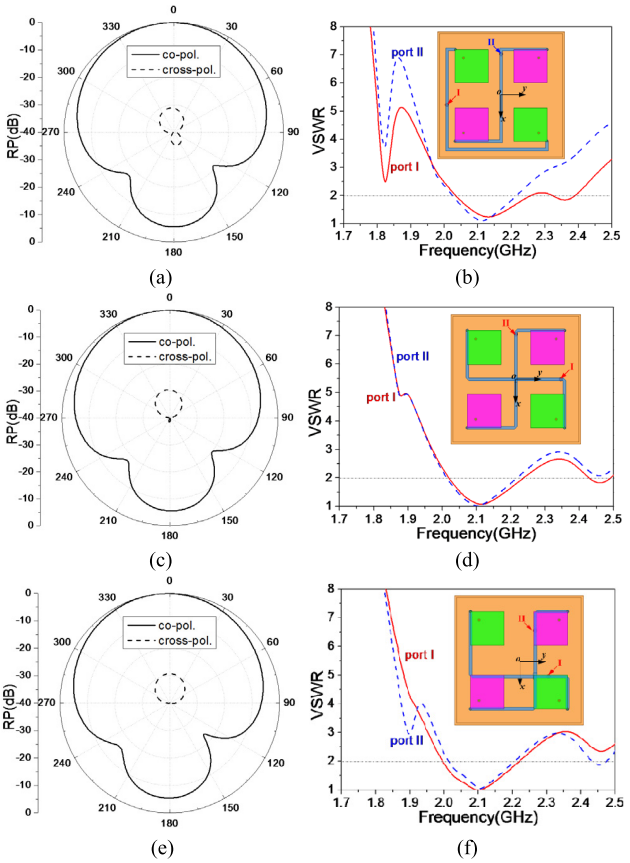

FIGURE 8. Performance of the antenna with three types of dual-polarized differential-fed networks. RPs (a) No-cross. (c) Center-cross. (e) Side-cross. and VSWRs (b) No-cross. (d) Center-cross. (f) Side-cross.

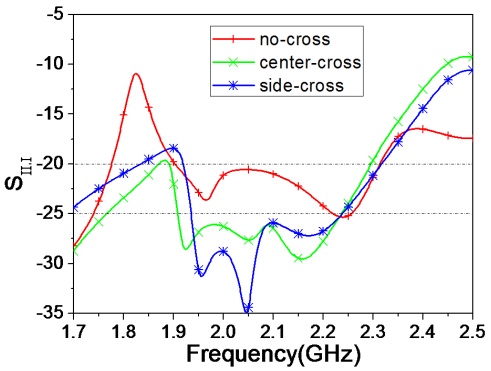

FIGURE 9. $S_{II,I}$ of three types of dual-polarized differential-fed networks with the antenna.

the same size, thereby making the dual polarizations operate at the same frequency bands. In some applications, different frequency bands at dual polarizations are also desired. When adopting different sizes of the micro patches in two diagonals and adjusting the radii and positions of the corresponding shorting poles, different frequency bands can be acquired for dual polarizations. In the experiment, a wide-beamwidth dual-polarized distributed microstrip antenna operating at different frequency bands are designed and manufactured.

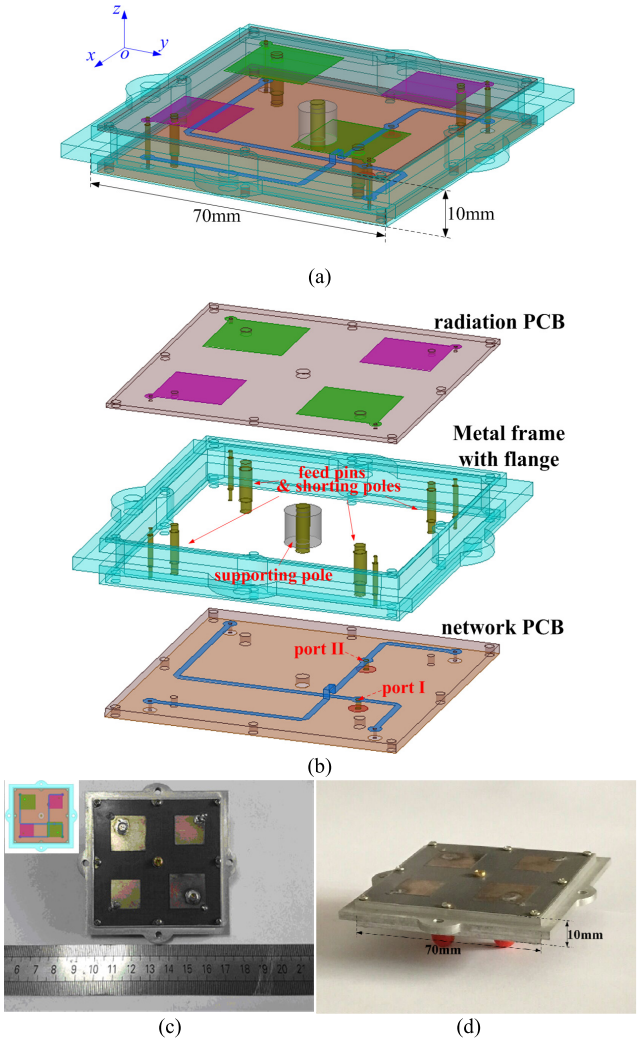

FIGURE 10. Experiment antenna. (a) 3D view of the model. (b) Exploded view of the model. (c) Top view of the prototype. (d) 3D view of the prototype.

A. DESIGN AND MANUFACTURE

The 3D view and the exploded view of the antenna are displayed in Fig. 10(a) and 10(b). The components of the antenna include a radiation PCB, a metal frame with flange, four feeding pins and four shorting poles, a supporting pole,

and a network PCB. The radiation PCB is acted as the support of four micro patches. Two pairs of micro patches respectively adopt different lengths for different frequencies of 2GHz and 2.2GHz. The radiation PCB is installed on the top of the metal frame, and the network PCB is installed on the bottom of that. These three components make the antenna form a closed cavity, so the antenna structure is robust. A flange extending from the metal frame is employed for installation purpose. Because of the metal frame, the antenna performance is not susceptible when it is mounted on an air platform. Some insulation materials can be placed between the antenna and the platform so that the effect of the platform on the antenna performance can be alleviated further. At the inside of the antenna, two pairs of shorting poles are settled respectively with desired positions and diameters for good impedance matching. At the center of the frame, a 8mm-diameter PTFE cylinder (ε_r =2.2) is adopted as supporting pole between the radiation PCB and network PCB, and a 3mm-diameter metal bolt is used to fix it with the two PCBs.

TABLE 2. Parameters of the proposed antenna.

Parameters	Meaning	Pol. I	Pol. II
L_p (mm)	Side length of the micro patch	17.8	15.8
r_s (mm)	Radius of the shorting pole	1.2	0.8
P_s (mm)	Position of the shorting pole	17.6	16.7
p_f (mm)	Position of the port	9.5	11.5
D_p (mm)	Space between micro patches	17	
X_c (mm) [a]	X coordinate of the cross	9.5	
Y_c (mm) [a]	Y coordinate of the cross	9.5	

[a] Origin of the coordinate system is located at the center of the antenna.

The prototype of the antenna is manufactured according to the above structure, and the photos are shown in Fig. 10(c) and 10(d). The materials of the two PCBs are both PTFE glass-fabric plate with a relative permittivity of 2.65 and a loss tangent of 0.002. Their thickness are 1mm and 2mm respectively. The metal frame with flange is milled with aluminum alloy. The thickness of the frame is 10mm, and the length excluding the flange is 70mm. The two PCBs are embedded into the top and the bottom of the metal frame and fixed by some small bolts. The RF connector is the pin-inserting SMA type, and the diameter of the pin is ∼1.2mm. The parameters of the antenna are listed in Table 2.

B. RESULT AND DISCUSSION

The performance of the experiment antenna is measured and compared with the calculated results. The measured data are acquired by a vector network analyzer (Agilent E8363B) and a far-field measurement system in an anechoic chamber. Fig. 11 shows the VSWRs of the two ports. The measured curves agree well with the calculated ones. The center frequencies of the two ports are well located at 2GHz and 2.2GHz respectively. The measured impedance bandwidths for VSWR≤2 are 9.2% (1.918∼2.102GHz) and 9.9% (2.108∼2.326GHz) respectively. Fig. 12 shows the coupling of the two ports versus frequency. The measured curve has the same variation trend with the calculated one.

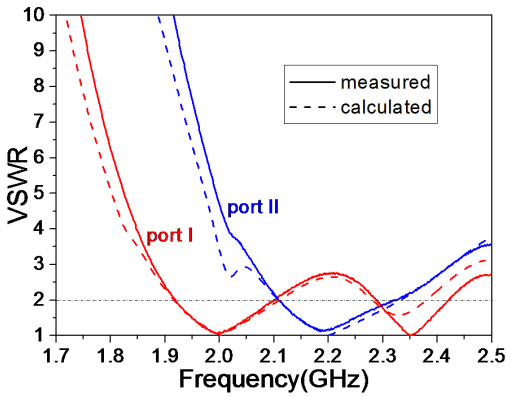

FIGURE 11. VSWRs of the experiment antenna.

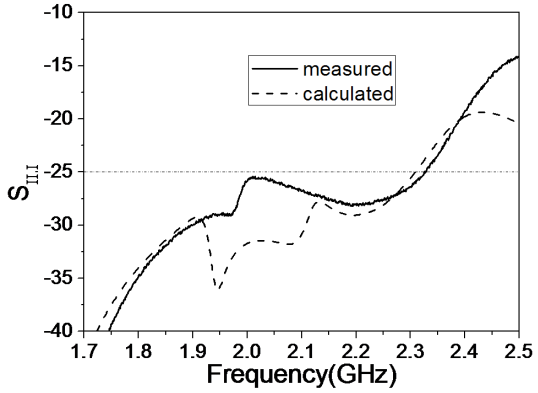

FIGURE 12. $S_{II,I}$ of the experiment antenna.

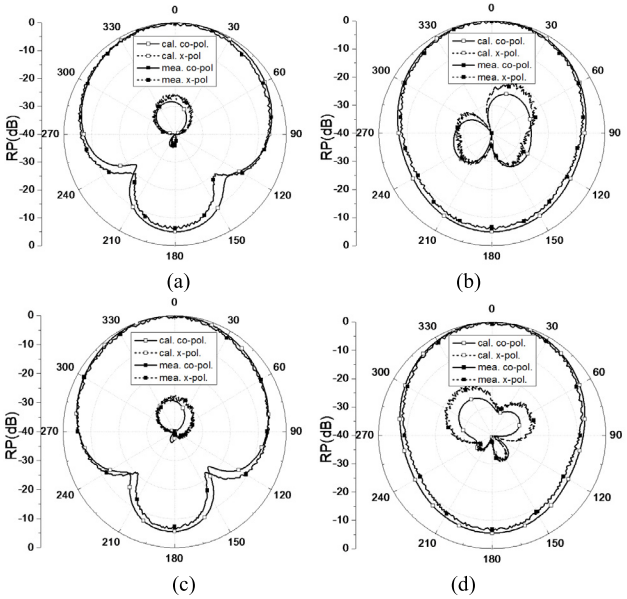

FIGURE 13. Measured and calculated RPs. Port I (a) E plane. (b) H plane. and Port II (c) E plane. (d) H plane.

In the whole operating band of 1.9∼2.3GHz, the measured $S_{II,I}$ is less than −25.4dB.

The radiation properties of the two polarizations are measured respectively at 2GHz and 2.2GHz. Fig. 13 shows the

TABLE 3. Antenna performance.

Terms	Port I (@ 2GHz)				Port II (@ 2.2GHz)			
	Gain (dB)	E-plane 3dB BW (°)	H-plane 3dB BW (°)	X-pol. (dB) @ θ=0°	Gain (dB)	E-plane 3dB BW (°)	H-plane 3dB BW (°)	X-pol. (dB) @ θ=0°
Cal.	5.2	118	95	-28.9	5.4	116	95	-29.4
Mea.	5.15	116	94	-26.2	5.5	115	93	-27.8
Terms	Imp. BW (port I)		Imp. BW (port II)		$S_{II,I}$ (dB) in 1.9~2.3GHz		Dimensions (L×H) @ 2.1GHz	
Cal.	9.7%		10.2%		≤-25.6		70mm×10mm	
Mea.	9.2%		9.9%		≤-25.4		0.49λ×0.07λ	

measured and calculated radiation patterns of the two polarizations in E plane and H plane. The measured results agree well with the calculated ones. The wide-beamwidth properties are both acquired in E plane for the two polarizations. The measured 3dB beamwidths in E plane are 116° and 115°, and those in H plane are 95° and 93°. Because cross polarization is easy to be affected by the fabricating and testing disturbances, the measured cross polarization values are slightly greater than the calculated ones, and the values in the normal direction are −26.3dB and −27.8dB respectively. In all directions, the values are all less than −20dB. The measured gains of the two polarizations are 5.15dB and 5.3dB respectively. All the detailed comparisons between measured and calculated data are listed in Table 3.

VI. CONCLUSIONS

A novel low-profile dual-polarized distributed microstrip antenna is proposed and studied. Because of the four micro patches adopted as the radiation component, wide beamwidths are acquired at dual polarizations by increasing the distance between the micro patches. The configuration, principle and design method of the antenna are presented in the paper. Compact dual-polarized differential-fed networks are discussed for the better performance of the antenna. To validate the feasibility of the proposed methods, a wide-beamwidth dual-polarized distributed microstrip antenna operating in different frequency bands is manufactured and measured. The dimensions of the antenna is $0.49\lambda \times 0.07\lambda$. The experiment results indicate the dual polarizations operate clearly in two different bands, and the impedance bandwidths reach 9.2% and 9.9% respectively. The acquired 3dB beamwidths in E plane are both over 115°, which are significantly greater than those of other reported ones. Meanwhile, the cross polarizations are less than −26.2dB, and the port isolation is more than 25.4dB. The proposed dual-polarized antenna successfully meet the requirements of both low profile and wide beamwidth, making it very attractive to the applications of airborne communication.

Furthermore, based on the analysis of the bandwidth of the micro patches shown in Section III, it is known the antenna also has a potential of wide bandwidth, i.e. the relative bandwidth of 16.5%. If wideband differential-feed networks are adopted, a more wideband property of the distributed microstrip antenna may be also obtained. This could be the next-step work.

ACKNOWLEDGMENT

The authors wish to thank China Scholarship Council (CSC) for the support of visiting scholar.

REFERENCES

[1] Q. X. Chu, D. L. Wen, and Y. Luo, "A broadband ±45° dual-polarized antenna with Y-shaped feeding lines," *IEEE Trans. Antennas Propag.*, vol. 63, no. 2, pp. 483–490, Aug. 2015.

[2] Y. Luo, Q. X. Chu, and D. L. Wen, "A plus/minus 45 degree dual-polarized base-station antenna with enhanced cross-polarization discrimination via addition of four parasitic elements placed in a square contour," *IEEE Trans. Antennas Propag.*, vol. 64, no. 4, pp. 1514–1519, Apr. 2016.

[3] L. Ge and K. M. Luk, "Linearly polarized and dual-polarized magneto-electric dipole antennas with reconfigurable beamwidth in the H-plane," *IEEE Trans. Antennas Propag.*, vol. 64, no. 2, pp. 423–431, Feb. 2016.

[4] H. Lee and B. Lee, "Compact broadband dual-polarized antenna for indoor MIMO wireless communication systems," *IEEE Trans. Antennas Propag.*, vol. 64, no. 2, pp. 766–770, Feb. 2016.

[5] C. X. Mao, S. Gao, Y. Wang, and F. Qin, "Multimode resonator-fed dual-polarized antenna array with enhanced bandwidth and selectivity," *IEEE Trans. Antennas Propag.*, vol. 63, no. 12, pp. 5492–5499, Dec. 2015.

[6] S. S. Zhong, Z. Sun, L. B. Kong, C. Gao, W. Wang, and M. P. Jin, "Tri-band dual-polarization shared-aperture microstrip array for SAR applications," *IEEE Trans. Antennas Propag.*, vol. 60, no. 9, pp. 4157–4165, Sep. 2012.

[7] P. K. Mishra, D. R. Jahagirdar, and G. Kumar, "A review of broadband dual linearly polarized microstrip antenna designs with high isolation [education column]," *IEEE Antennas Propag. Mag.*, vol. 56, no. 6, pp. 238–251, Dec. 2014.

[8] Y. Gou, S. Yang, J. Li, and Z. Nie, "A compact dual-polarized printed dipole antenna with high isolation for wideband base station applications," *IEEE Trans. Antennas Propag.*, vol. 62, no. 8, pp. 4392–4395, Aug. 2014.

[9] Y. Cui, R. Li, and H. Fu, "A broad dual-polarized planar antenna for 2G/3G/LTE base stations," *IEEE Trans. Antennas Propag.*, vol. 62, no. 9, pp. 4836–4840, Sep. 2014.

[10] Q. Xue, S. W. Liao, and J. H. Xu, "A differentially-driven dual-polarized magneto-electric dipole antenna," *IEEE Trans. Antennas Propag.*, vol. 61, no. 1, pp. 425–430, Jan. 2013.

[11] B. Q. Wu and K. M. Luk, "A broadband dual-polarized magneto-electric dipole antenna with simple feeds," *IEEE Antennas Wireless Propag. Lett.*, vol. 8, pp. 60–63, Dec. 2009.

[12] L. Siu, H. Wong, and K. M. Luk, "A dual-polarized magneto-electric dipole with dielectric loading," *IEEE Trans. Antennas Propag.*, vol. 57, no. 3, pp. 616–623, Mar. 2009.

[13] J. Li, S. Yang, Y. Gou, and J. Hu, "Wideband dual-polarized magnetically coupled patch antenna array with high port isolation," *IEEE Trans. Antennas Propag.*, vol. 64, no. 1, pp. 117–125, Jan. 2016.

[14] J. Y. Deng, L. X. Guo, Y. Z. Yin, J. Qiu, and Z. S. Wu, "Broadband patch antennas fed by novel tuned loop," *IEEE Trans. Antennas Propag.*, vol. 61, no. 4, pp. 2290–2293, Apr. 2013.

[15] Y. X. Guo, K. W. Khoo, and L. C. Ong, "Wideband dual-polarized patch antenna with broadband baluns," *IEEE Trans. Antennas Propag.*, vol. 55, no. 1, pp. 78–83, Jan. 2007.

[16] K. L. Wong and T. W. Chiou, "Broad-band dual-polarized patch antennas fed by capacitively coupled feed and slot-coupled feed," *IEEE Trans. Antennas Propag.*, vol. 50, no. 3, pp. 346–351, Mar. 2002.

[17] K. B. Ng, C. H. Chan, and K. M. Luk, "Low-cost vertical patch antenna with wide axial-ratio beamwidth for handheld satellite communications terminals," *IEEE Trans. Antennas Propag.*, vol. 63, no. 4, pp. 1417–1424, Apr. 2015.
[18] H. He, "A novel wide beam circular polarization antenna—Microstrip-dielectric antenna," in *Proc. ICMMT*, 2002, pp. 381–384.
[19] Z. K. Pan, W. X. Lin, and Q. X. Chu, "Compact wide-beam circularly-polarized microstrip antenna with a parasitic ring for CNSS application," *IEEE Trans. Antennas Propag.*, vol. 62, no. 5, pp. 2847–2850, May 2014.
[20] L. Chen, T. L. Zhang, C. Wang, and X. W. Shi, "Wideband circularly polarized microstrip antenna with wide beamwidth," *IEEE Antennas Wireless Propag. Lett.*, vol. 13, pp. 1577–1580, Jul. 2014.
[21] C. W. Su, S. K. Huang, and C. H. Lee, "CP microstrip antenna with wide beamwidth for GPS band application," *Electron. Lett.*, vol. 43, no. 30, pp. 1–2, Sep. 2007.
[22] W. R. Eisenstadt, B. Stengel, and B. M. Thompson, *Microwave Differential Circuit Design Using Mixed-Mode S-Parameters*, vols. 42–45. Boston, MA, USA: Artech House, 2006, pp. 1–25.
[23] H. Jin, K. S. Chin, W. Che, and C. C. Chang, "Differential-fed patch antenna arrays with low cross polarization and wide bandwidths," *IEEE Antennas Wireless Propag. Lett.*, vol. 13, pp. 1069–1072, Jun. 2014.

XI CHEN, photograph and biography not available at the time of publication.

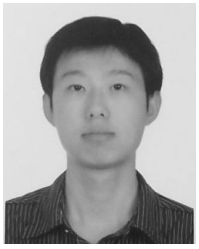

PEI-YUAN QIN was born in Liaoning, China, in 1983. He received the bachelor's degree in electronic engineering from Xidian University, Xi'an, China, in 2006, and a joint Ph.D. degree in electromagnetic fields and microwave technology from Xidian University and Macquarie University, Australia, in 2012.

From 2012 to 2015, he was a Post-Doctoral Research Fellow with the Commonwealth Scientific and Industrial Research Organisation, Australia. From 2015 to 2016, he was a Chancellor's Post-Doctoral Research Fellow/Lecturer with the University of Technology Sydney, Australia, where he has been a Senior Lecturer, since 2017. His research interests include reconfigurable antennas, phase shifters, reconfigurable reflectarrays, and MIMO communications.

Dr. Qin was a recipient of the Australia Research Council Discovery Early Career Researcher Award. He was a recipient of the International Macquarie University Research Excellence Scholarship and the Vice-Chancellor's Commendation for academic excellence by Macquarie University. One of his papers was selected as the 2016 Computer Simulation Technology University Publication Award.

Y. JAY GUO (F'14) received the bachelor's and master's degrees from Xidian University in 1982 and 1984, respectively, and the Ph.D. degree from Xian Jiaotong University in 1987.

He held various senior strategic leadership positions at Fujitsu, Siemens, and NEC in the U.K. In 2014, he served as a Research Director with CSIRO, for over nine years, directing a number of ICT research portfolios. He is currently a Distinguished Professor and the Founding Director of the Global Big Data Technologies Centre, University of Technology Sydney, Australia. He has authored over 300 academic research papers, three books and numerous book chapters, and holds over 20 international patents. His research interests include antennas, mm-wave and THz communications, and sensing systems.

Dr. Guo has chaired numerous international conferences. He is the International Advisory Committee Chair of the IEEE VTC2017, the General Chair of ISAP2015, iWAT2014, and WPMC'2014, and the TPC Chair of the 2010 IEEE WCNC, and the 2012 and 2007 IEEE ISCIT. He serves as a Guest Editor of the IEEE TRANSACTIONS ON ANTENNAS AND PROPAGATION, special issues on Antennas for Satellite Communications and Antennas and Propagation Aspects of 60–90 GHz Wireless Communications, the IEEE JOURNAL ON SELECTED AREAS IN COMMUNICATIONS, special issue on Communications Challenges and Dynamics for Unmanned Autonomous Vehicles, and the *IEEE Network Magazine*, special issue on 5G for Mission Critical Machine Communications. He is a fellow of the Australian Academy of Engineering and Technology and the IET, and a member of the College of Experts of Australian Research Council. He received a number of most prestigious Australian national awards, and was named one of the most influential engineers in Australia in 2014 and 2015.

GUANG FU, photograph and biography not available at the time of publication.